Received: 27 February 2019 | Revised: 17 October 2019 | Accepted: 25 October 2019

DOI: 10.1002/glia.23748

GLIA

WILEY

RESEARCH ARTICLE

Epigenetic regulation of microglial phosphatidylinositol 3-kinase pathway involved in long-term potentiation and synaptic plasticity in rats

Genevieve Saw[1] | Kumar Krishna[2] | Neelima Gupta[1] | Tuck Wah Soong[2] | Karthik Mallilankaraman[2] | Sreedharan Sajikumar[2] | S. Thameem Dheen[1]

[1]Department of Anatomy, Yong Loo Lin School of Medicine, National University of Singapore, Singapore

[2]Department of Physiology, Yong Loo Lin School of Medicine, National University of Singapore, Singapore

Correspondence

S. Thameem Dheen, Department of Anatomy, Yong Loo Lin School of Medicine, National University of Singapore, Singapore 117597.
Email: antstd@nus.edu.sg

Sreedharan Sajikumar, Department of Physiology, Yong Loo Lin School of Medicine, National University of Singapore, Singapore 117597.
Email: phssks@nus.edu.sg

Abstract

Microglia are the main form of immune defense in the central nervous system. Microglia express phosphatidylinositol 3-kinase (PI3K), which has been shown to play a significant role in synaptic plasticity in neurons and inflammation via microglia. This study shows that microglial PI3K is regulated epigenetically through histone modifications and posttranslationally through sumoylation and is involved in long-term potentiation (LTP) by modulating the expression of brain-derived neurotrophic factor (BDNF), which has been shown to be involved in neuronal synaptic plasticity. Sodium butyrate, a histone deacetylase inhibitor, upregulates PI3K expression, the phosphorylation of its downstream effectors, AKT and cAMP response element-binding protein (CREB), and the expression of BDNF in microglia, suggesting that BDNF secretion is regulated in microglia via epigenetic regulation of PI3K. Further, knockdown of SUMO1 in BV2 microglia results in a decrease in the expression of PI3K, the phosphorylation of AKT and CREB, as well as the expression of BDNF. These results suggest that microglial PI3K is epigenetically regulated by histone modifications and posttranslationally modified by sumoylation, leading to altered expression of BDNF. Whole-cell voltage-clamp showed the involvement of microglia in neuronal LTP, as selective ablation or disruption of microglia with clodronate in rat hippocampal slices abolished LTP. However, LTP was rescued when the same hippocampal slices were treated with active PI3K or BDNF, indicating that microglial PI3K/AKT signaling contributes to LTP and synaptic plasticity. Understanding the mechanisms by which microglial PI3K influences synapses provides insights into the ways it can modulate synaptic transmission and plasticity in learning and memory.

KEYWORDS

histone deacetylase, long-term potentiation, microglia, sumoylation, synaptic plasticity

1 | INTRODUCTION

Glial cells are the non-neuronal cells in the central nervous system (CNS) consisting mainly of astrocytes, microglia, and oligodendrocytes (Jäkel & Dimou, 2017). They have long known to be involved in housekeeping activities within the brain, providing support, protection, and maintaining homeostasis. Recent studies have shown that contrary to popular belief, glial cells may play important role in regulating synaptic transmission, synaptic plasticity, and thus memory formation (Hertz & Chen, 2016; Pfeiffer, Avignone, & Nägerl, 2016).

Microglia, which account for 5–12% of the total glia population (Norden & Godbout, 2013), function as the immune cells of the brain and serve as the main line of defense when there is an injury, insult, or pathogenic infiltration in the CNS. In addition, microglia play a vital role in pruning weaker synaptic connections during brain development (Hong, Dissing-Olesen, & Stevens, 2016). They secrete cytokines and chemokines that bring about a pro-inflammatory environment and also phagocytose dead cells and debris ensuring a favorable environment for neurons. Microglia in the adult healthy brain appear to be ramified in morphology, and they survey the brain microenvironment and make contact with synapses. The activated microglia in response to injury or infection migrate to the site of insult, proliferate rapidly, become amoeboid in shape, and secrete chemokines and cytokines that can be pro-inflammatory or anti-inflammatory depending on the polarizing state of microglia (Ji, Akgul, Wollmuth, & Tsirka, 2013). M1 polarization promotes inflammation and results in the release of pro-inflammatory cytokines while M2 polarization suppresses inflammation and brings about the release of anti-inflammatory cytokines and is considered to be neuroprotective (Koellhoffer, Grenier, Ritzel, & McCullough, 2015).

It has been shown recently that microglia play an active role in synaptic transmission and possibly in the remodulation of synapses (Tremblay & Majewska, 2011; Wu, Dissing-Olesen, MacVicar, & Stevens, 2015) by regulating the number of functional synapses in the brain (Ji et al., 2013). This suggests a role for microglia in synaptic plasticity, which underlies learning and memory (Mayford, Siegelbaum, & Kandel, 2012; Neves, Cooke, & Bliss, 2008; Takeuchi, Duszkiewicz, & Morris, 2014). Microglial processes have been shown to be in contact with pre- and post-synaptic terminals as well as with astrocytes surrounding the synapse indicating that microglia may contribute to activity-dependent synaptic refinement or elimination. Microglia secrete factors such as BDNF (Gomes et al., 2013) and tumor necrosis factor alpha (TNFα) (Schafer, Lehrman, & Stevens, 2013), which may affect neurotransmission and subsequently synaptic plasticity. Recently, it has been shown that microglia are also able to change the number of synapses and dendrites (Kettenmann, Kirchhoff, & Verkhratsky, 2013; Pfeiffer et al., 2016). Microglia have been shown to be dystrophic in brains of patients with Alzheimer's disease (Streit, Braak, Xue, & Bechmann, 2009), where these cells cluster around amyloid beta (Aβ) plaques and limit the expansion of Aβ plaques and plaque-associated disruption of neuronal connection (Zhao et al. 2017). This suggests a role for microglia in neuropathological conditions ultimately affecting learning and memory.

Phosphatidylinositol 3-kinase (PI3K) is a lipid kinase that phosphorylates phosphoinositides at the 3′ position of the inositol ring and generates phosphatidylinositol (3,4,5)-trisphosphate. PI3K, which consists of p85α (regulatory subunit) and p110α (catalytic subunit), has been implicated in synaptic plasticity in neurons (Horwood, Dufour, Laroche, & Davis, 2006) and in the induction and maintenance of long-term potentiation (LTP) in the hippocampal CA1 region (Sui, Wang, & Li, 2008). PI3K is also expressed in microglia, and thus, this has intrigued us to explore the function of PI3K in microglia and to determine if microglial PI3K plays a role in synaptic transmission.

Downstream effectors of microglial PI3K include protein kinase B (AKT), cAMP response element-binding protein (CREB), and brain-derived neurotrophic factor (BDNF). Microglia have been shown to play a critical role in the formation of learning and memory by promoting synapse formation through BDNF signaling (Parkhurst et al., 2013). It has been proposed that PI3K in microglia may alter the expression and secretion of BDNF, which will in turn affect synaptic transmission between neurons and thus synaptic plasticity (Welberg, 2014).

Epigenetic mechanisms such as DNA methylation, histone modifications, and small microRNA (miRNA) regulation play an important role in the regulation of gene expression without altering gene sequence. Altered epigenetic mechanisms have been shown to be associated with many disease conditions (Egger, Liang, Aparicio, & Jones, 2004; Jones & Baylin, 2002; Kim, 2005; Moosavi & Ardekani, 2016). PI3K has been shown to be epigenetically regulated by histone modifications (Ellis et al., 2013; Iaconelli et al., 2017). Microglia have been shown to be regulated by histone deacetylases in development, homeostasis, and neurodegeneration, and the deletion of histone deacetylases 1 and 2 drastically altered microglial development and function. In mouse models of Alzheimer's disease, deletion of these histone deacetylases (HDACs) resulted in a decrease in amyloid plaques and improved cognitive impairment by augmenting microglial amyloid phagocytosis (Datta et al., 2018). This suggests a vital role for histone modifications in microglia with regard to memory and neurodegeneration. Therefore, we examined the epigenetic regulation of microglial PI3K by HDAC inhibition and its modulation on synaptic plasticity.

Sumoylation is a posttranslational modification by small ubiquitin-like modifier (SUMO) proteins, which regulates a range of different protein functions (Park-Sarge & Sarge, 2008). PI3K has been shown to be sumoylated in other cell types (De la Cruz-Herrera et al., 2016); however, sumoylation of PI3K has not yet been explored in microglia. Research on SUMO proteins and sumoylation in microglia has not been studied in detail. The SUMO pathway has emerged as a promising therapeutic target in recent years in areas such as cancer therapy (Bialik & Woźniak, 2017), myocardial ischemia (Du et al., 2018), and also for neuroprotection in brain ischemia (Yang, Sheng, & Wang, 2016). Since the PI3K/AKT pathway is affected by sumoylation, this study attempts to understand the role of sumoylation in microglia on the regulation of the pathway, BDNF expression and its effects on LTP, and synaptic plasticity. This study is the first of its kind, as we investigated the epigenetic and posttranslational modifications of

microglial PI3K altering synaptic transmission. Understanding how microglial factors regulate synapses and mediate synaptic plasticity may in turn be helpful in ameliorating cognitive impairments caused by dystrophic microglia in aging brains.

2 | MATERIALS AND METHODS

2.1 | Ethics statement

Wistar rats (1 day old, 5 days old, and 28 days old) were purchased from InVivos, Singapore. All procedures were carried out in accordance with the National University of Singapore Institutional Animal Care and Use Committee (IACUC) guidelines (NUS/IACUC/R14-1643). Thirty-seven 4-week-old male Wistar rats were used for whole-cell patch-clamp recordings. All efforts were made to minimize pain and number of animals used.

2.2 | Cell culture

BV-2 cells (a murine microglial cell line) were maintained in 75-cm^2 culture flasks in Dulbecco's Modified Eagle's Medium (DMEM) (Cat. no. SH30022.01, GE Healthcare, USA) supplemented with 10% fetal bovine serum (FBS) (Cat. no. SV30160.03, GE Healthcare, USA) and 1% antibiotic–antimycotic (Cat. no. A5955, Sigma-Aldrich, USA) solution. Cells were maintained at 37°C in a humidified atmosphere of 5% CO_2. Cells were seeded on 6-well plates with a density of about 1.0×10^6 per well. Experiments involving HDACi treatment consisted of BV2 cells treated with sodium butyrate (NaBu) (2.5 mM) (Cat. no. 303410, Sigma-Aldrich, USA) for 1 hr. Experiments with PI3K inhibitor LY294002 (Cat. No. 9901, Cell Signalling Technologies, USA) involved the treatment of cells with LY294002 (10 μM) for 1 hr, and the effect of inhibition was seen. For experiments involving both LY204002 and HDACi, cells were treated with LY294002 for 1 hr prior to NaBu treatment to allow the inhibition of PI3K to take effect. SUMO1 knockdown cells were incubated with active PI3K (1 μg/mL, Cat. no. P27-18H-10, SignalChem, Vancouver, Canada).

2.3 | Primary microglial culture

Brain tissue was isolated from 5-day-old postnatal rat pups from $n = 3$ families, and the meninges were removed. Mixed glial cells of the cerebrum were cultured in a flask containing medium comprising of DMEM/high glucose (Cat. no. SH30022.01; HyClone, USA), 10% FBS (Cat. no. SV30160.03; HyClone, USA), 10 mL/L antibiotic–antimycotic (Cat. no. A5955; Sigma-Aldrich, USA), 0.1 mM nonessential amino acid (Invitrogen, CA), and 1 mL/L insulin (Cat. no. I-0516; Sigma-Aldrich, USA). The complete medium was replaced after 24 hr and then every 3–4 days. Cultures were maintained for 10 days in a humidified incubator at 37°C and 5% CO_2 until confluence is achieved. Microglial cells were isolated with 0.25% trypsin containing 1 mM ethylenediaminetetraacetic acid for 10–20 min at 37°C (Saura, Tusell, & Serratosa, 2003) to obtain a culture of pure microglial cells.

2.4 | Western blot

Total protein was extracted from BV2 cell cultures using the MPER protein extraction reagent (Cat. no. 78501; Thermo Fisher, USA) containing protease and phosphatase inhibitors (Cat. nos. 88667 and 88665, Thermo Fisher, USA), and concentrations were analyzed using Bradford assay (Cat. no. 500–0006, Bio-Rad, USA). Thirty micrograms of protein was run on 4–15% Mini-PROTEAN TGX Precast Protein Gels (10 well) and transferred to polyvinylidene difluoride membranes. The membranes were subsequently blocked using 5% bovine serum albumin (BSA) or 5% milk, depending on the nature of the protein, and incubated with primary antibodies against PI3K (1:1000, Cat. No. 4255; Cell Signaling Technologies, USA), phosphorylated AKT at Ser473 (1:1000, Cat. No. 9271; Cell Signaling Technologies, USA), AKT (1:1000, Cat. No. 9272; Cell Signaling Technologies, USA), phosphorylated CREB at Ser133 (1:1000, Cat. No. 9198; Cell Signaling Technologies, USA), CREB (1:1000, Cat. No. 4820; Cell Signaling Technologies, USA), and BDNF (1:1000, Cat. No. ab205067; Abcam, UK) individually prepared in 5% BSA in Tris-buffered saline, 0.1% Tween 20 (TBST) overnight at 4°C. Blots were subsequently incubated with horseradish peroxidase-conjugated secondary antibodies in either 5% BSA or milk for 1 hr at room temperature. Blots were developed with the chemiluminescence detection system (Cat. no. 34078, SuperSignal West Pico Chemiluminescent Substrate; Thermo Fisher, USA), exposed on X-ray films. Signal intensity was determined using Quantity One Software (Bio-Rad).

2.5 | Generation of stable SUMO1 knockdown cell lines

Five different lentiviruses carrying short hairpin RNAs (shRNAs) targeting different regions of SUMO1 were produced by co-transfecting 293T/17 cells with SUMO1 lentiviral shRNA constructs (Dharmacon, USA), pMDLg/pRRE (Addgene Plasmid #12251, USA), pRSV-Rev (Addgene Plasmid #12253, USA), and pMD2.G (Addgene Plasmid #12259, USA), as described previously with slight modifications (Mallilankaraman, Cárdenas, et al., 2012; Mallilankaraman, Doonan, et al., 2012). BV2 microglial cells (5×10^5/well) grown in 6-well plates were transduced with SUMO1 lentiviruses, selected with puromycin (2ug/ml) 48 hr posttransduction for 6–10 days, and expanded. Knockdown of SUMO1 in microglia was assessed by western blotting of the SUMO1 protein.

2.6 | Chromatin immunoprecipitation

Chromatin immunoprecipitation (ChIP) was performed using EZ-ChIP Chromatin Immunoprecipitation Kit (Cat. no. 17–371; Merck Millipore, USA) according to manufacturer's guidelines. Protein–DNA were

crosslinked in cultured BV2 microglial cells with 1% paraformaldehyde (PFA) for 10 min after which the reaction was quenched using 2.5 mM glycine. The cells were lysed on ice, and the crude extracts were sonicated (Bioruptor, Diagenode) to shear crosslinked DNA into smaller fragments (200–1,000 bp) and visualized by gel electrophoresis. This was followed by incubating the sheared DNA with Protein A Agarose/Salmon Sperm (Cat. no. 16–157, Merck Millipore, USA) beads to preclear nonspecific interactions. Subsequently, aliquots were incubated under shaking with relevant antibody H3K9ac (Cat. no. 07–352, Merck Millipore, USA) and IgG (Cat. no. SC2027 X, Santa Cruz, USA) at 4°C, overnight. Protein A Agarose/Salmon Sperm beads were used to pull down antibody-bound protein–DNA and treated to subsequent washes before elution. Crosslinking was then reversed, and the immunoprecipitated DNA fragments were purified using the QIAquick PCR purification Kit (Cat. no. 28,104, Qiagen, Germany) and amplified. The samples were then run through a quantitative real-time polymerase chain reaction (qPCR) using primers for Pik3ca and analyzed with reference to 1% input DNA (sample without antibody pull down). Rabbit IgG served as negative control to verify reaction specificity. Primers were synthesized for Pik3ca and positive ChIP control, glyceraldehyde 3-phosphate dehydrogenase (GAPDH) (sequences provided). Commercially available primers were used as the negative control for ChIP analysis (Mouse Negative Control Primer Set 1, Cat no. 71011, Active Motif, USA).

List of primer sequences used for the study:

Pik3ca_Chip_For: 5′CTCAGTGCTGTCGTCAGTGT3′.

Pik3ca_Chip_Rev: 5′GCTCTGACCCTCTGCAAACT3′.

Gapdh_Chip_For: 5′CCTCTGCGCCCTTGAGCTAGG3′.

Gapdh_Chip_Rev: 5′CACAAGAAGATGCGGCCGTCTC3′.

2.7 | Immunocytochemistry

Primary microglia and BV2 cells were cultured on 13-mm glass coverslips and fixed using 4% PFA for 15 min and blocked with 5% goat serum for 1 hr. The cells were incubated at 4°C overnight in primary antibody against PI3K (1:100, Cat. No. 4255; Cell Signaling Technologies, USA), phosphorylated AKT at Ser473 (1:100, Cat. No. 9271; Cell Signaling Technologies, USA), AKT (1:100, Cat. No. 9272; Cell Signaling Technologies, USA), phosphorylated CREB at Ser133 (1:100, Cat. No. 9198; Cell Signaling Technologies, USA), CREB (1:100, Cat. No. 4820; Cell Signaling Technologies, USA), and BDNF (1:100, Cat. No. ab205067; Abcam, UK). Secondary antibodies were incubated for 1 hr at room temperature, and coverslips were counterstained with 4′,6-diamidino-2-phenylindole (DAPI) (1 μg/mL, Cat. No. D1306; Invitrogen, USA) for 5 min and then mounted with fluorescent mounting medium (DakoCytomation, Glostrop, Denmark). Slides were allowed to dry for at least one day before imaging. Images were taken using LSM FV1000 (Olympus, Japan).

2.8 | Immunohistochemistry

Twenty-eight-day old Wistar rats were perfused and fixed with 4% PFA for further procedure. For double immunofluorescence staining, forebrain sections at 30 μm were cut through the corpus callosum using a cryostat (Model No. CM 3050 S; Leica Microsystems GmbH, Wetzlar, Germany). The sections were treated with 0.2% Triton-X 100 and blocked in 3% BSA and then incubated with primary antibodies overnight at 4°C. On the following day, the sections were further incubated with either FITC- or Cy3-conjugated secondary antibodies. The sections were counterstained with DAPI (1 μg/mL, Cat. No. D1306; Invitrogen, USA) and mounted with a fluorescent mounting medium (DakoCytomation, Glostrop, Denmark). Images were taken using LSM FV1000 (Olympus, Japan).

2.9 | Preparation of hippocampal slices for whole-cell voltage-clamp recordings

All experiments were performed on acute transverse hippocampal slices from 4-week-old male Wistar rats (60 slices from 37 rats). CO_2 was used for anesthetization, and brains were rapidly removed after decapitation and placed in ice-cold oxygenated artificial cerebrospinal fluid (ACSF) containing the following (in mM): 206 sucrose, 2.8 KCl, 1 $MgCl_2$, 1 $CaCl_2$, 2 $MgSO_4$, NaH_2 PO_4, $NaHCO_3$, 10 glucose, and 0.4 ascorbic acid, pH 7.3, 95% O_2/5% CO_2. Slices were cut at a thickness of 350 μm using a vibratome (VT1200S; Leica Biosystems) and immediately transferred to an incubation chamber filled with ACSF containing the following (in mM): 124 NaCl, 3.7 KCl, 1.2 KH_2PO_4, 1 $MgSO_4.7H_2O$, 2.5 $CaCl_2{\cdot}2H_2O$, 24.6 $NaHCO_3$, and 10 D-glucose, pH 7.3, equilibrated with to 95% O_2 and 5% CO_2. Slices were allowed to recover at 32°C for 1 h and were then maintained at room temperature. Picrotoxin (100 μM) was added to the bath medium in all experiments to block the action of gamma-aminobutyric acid (GABA) receptors (Krishna, Behnisch, & Sajikumar, 2016).

2.10 | Whole-cell voltage-clamp recordings

Whole-cell voltage-clamp recordings of evoked excitatory postsynaptic currents (EPSCs) were generated from the soma of visually identified pyramidal neurons located within the CA1 region of the hippocampus (Krishna et al., 2016). Patch pipettes (4–6 MΩ) were filled with internal solution containing the following (in mM): 135 $CsMeSO_3$, 8 NaCl, 10 HEPES, 0.25 EGTA, $2Mg_2ATP$, $0.3Na_3GTP$, 0.1 spermine, 7 phosphocreatine, and 5QX-314 (pH 7.3). Series (access) resistance was within the range of 15–35 M throughout each experiment. Access resistance, membrane resistance, and membrane capacitance were monitored to ensure the stability and the health of cells during the experiment. Recordings were considered stable when the membrane resistance, membrane capacitance, and holding current did not change more than 20%.

Neurons were held at a holding potential of −70 mV. The triple patch-clamp EPC10 patch-clamp amplifier and software Patch-master (HEKA Electronics, Lambrecht, Germany) were used for data acquisition. In addition, a CED 1401 analog to digital converter (Cambridge Electronic Design, UK) and a custom-made software program were used to regulate stimulation and to record evoked EPSCs.

EPSCs were evoked by stimulation of Schaffer-collateral fibers in the stratum radiatum (str. Rad.) using tungsten-stimulating electrode (AM Systems, WA, Australia). Schaffer collateral/commissural projections were stimulated at 0.05 Hz by 200 μs voltage pulses generated by an isolated pulse stimulator (Model 2100, AM Systems). The stimulation strength (2–5 V) was adjusted to evoke EPSCs with amplitude of approximately 50 pA. Basal synaptic currents were recorded for at least 10 min prior to LTP induction. LTP was induced within 10 min after whole-cell break-in by a 1 S, 100 Hz stimulation burst (high frequency stimulation) synchronized with a depolarization to 0 mV for 2 s through the patch pipette. The slope of EPSCs was measured to analyze the change in synaptic transmission before and after induction of LTP in CA1 pyramidal cells. The EPSC slope values were normalized to the first 5 min of EPSC recording. (Krishna et al., 2016)

Slices were incubated with clodronate liposomes (100 μg/mL, Clodrosome®; Encapsula NanoSciences, USA) for 90 min prior to recording. Control slices were incubated with control liposomes (100 μg/mL, Encapsome®; Encapsula NanoSciences, USA) not containing clodronate. Clodronate-incubated hippocampal slices were then incubated with either active PI3K (1 μg/mL, Cat. No. P27-18H-10; SignalChem, USA) or BDNF (200 ng/mL, Cat. No. 3897; Cell Signalling Technologies, USA) 20 min before cells were patched.

2.11 | Preparation of hippocampal slices for field recording studies

A total of 22 hippocampal slices from 10 male Wistar rats (5–7 weeks old) were used for field recording studies. Rats were maintained on a 12/12 hr light dark cycle, with food and water available ad libitum. Animals were decapitated after anesthetization using CO_2, and the brains were quickly transferred into cold (2–4°C) ACSF. The ACSF contained the following (in mM): 124 NaCl, 3.7 KCl, 1.2 KH_2PO_4, 1 $MgSO_4{\cdot}7H_2O$, 2.5 $CaCl_2{\cdot}2H_2O$, 24.6 $NaHCO_3$, and 10 D-glucose, pH 7.3, and equilibrated with to 95% O_2 and 5% CO_2 (carbogen; total consumption 16 L/h). From each male Wistar rat, 8–10 transverse slices from the right hippocampus (400 μm thick) were prepared using a tissue chopper. The slices were incubated at 32°C in an interface chamber (Scientific System Design) with ACSF flow rate of 1 mL/min. Field EPSP recordings and stimulations were carried out using the procedures described earlier (Krishna et al., 2016). Slices were incubated with clodronate liposomes (100 μg/mL, Clodrosome®, Encapsula NanoSciences, USA) for 90 min prior to recording. Slices were then perfused with conditioned media form BV2 cells (control, HDACi-treated, and SUMO1 knockdown) for 2 hr before baseline recording. Late-LTP was induced using three stimulus trains of 100 pulses ("strong" tetanus [STET], 100 Hz; duration, 0.2 ms/polarity; intertrain interval, 10 min).

2.12 | MTS assay

In order to evaluate the toxicity of HDAC inhibitor, NaBu on viability of BV2 cells, an MTS assay was performed. About 10,000 BV2 cells were seeded in 96-well plates and incubated at 37°C. Twenty microliters of 3-(4,5-dimethylthiazol-2-yl)-5-(3-carboxymethoxyphenyl)-2-(4-sulfophenyl)-2H-tetrazolium (MTS) reagent (Promega, Cat No. G358C, USA) was added to each well, and cells were treated with NaBu (2.5 mM). Absorbance was read at 490 nm in a 96-well plate reader at time points of 0 (before treatment) to 6 hr posttreatment.

2.13 | Statistical analyses

Experiments were performed using 3–4 biological replicates, independently replicated. The data are represented as mean ± *SEM*, and Student's *t* test was done using Microsoft Excel. The results were considered significant when $p < .05$. LTP values were analyzed using the Wilcoxon signed rank test when compared within the group while Mann–Whitney *U* test was used when comparing data between groups.

3 | RESULTS

It is known that microglia express genes involved in synaptic plasticity in neurons (Beppu et al., 2013; Slepko, Patrizio, & Levi, 1999; Stebbing, Cottee, & Rana, 2015). Neuronal PI3K is a key player in the occurrence of LTP. Therefore, this study was aimed to investigate if the PI3K expressed in microglia has any role in LTP.

3.1 | The expression of PI3K in microglia

The expression of PI3K in microglia was confirmed by immunofluorescence staining in both BV2 microglial cells and rat primary microglia (Figure 1a) and by western blot (Figure 1b). PI3K expression was detected largely in the cytoplasm of microglia.

3.2 | Epigenetic regulation of microglial PI3K by histone modifications

Since PI3K has been shown to be regulated by histone modifications, BV2 microglial cells were treated with NaBu, a histone deacetylase inhibitor (HDACi) for 1 hr and the resulting levels of PI3K protein expression were quantified. Upon HDACi treatment, PI3K levels were significantly upregulated in microglia (Figure 2a,b, $p = .0102$). In addition, there was also an increase in the PI3K-dependent phosphorylation of AKT ($p = .0031$) and CREB ($p = .0011$), while the levels of total AKT and total CREB remained unchanged, suggesting that the PI3K-AKT-CREB signaling pathway is regulated by histone modifications. As CREB has been shown to be a key mediator of BDNF-induced gene expression (Finkbeiner et al. 1997), this study further revealed that HDACi-induced activation of PI3K-AKT-CREB signaling pathway upregulated the BDNF expression significantly in microglia (Figure 2a,b, $p = .0154$). In order to confirm the effect of HDAC inhibition on BDNF was mediated via PI3K signaling, the cells were co-treated with

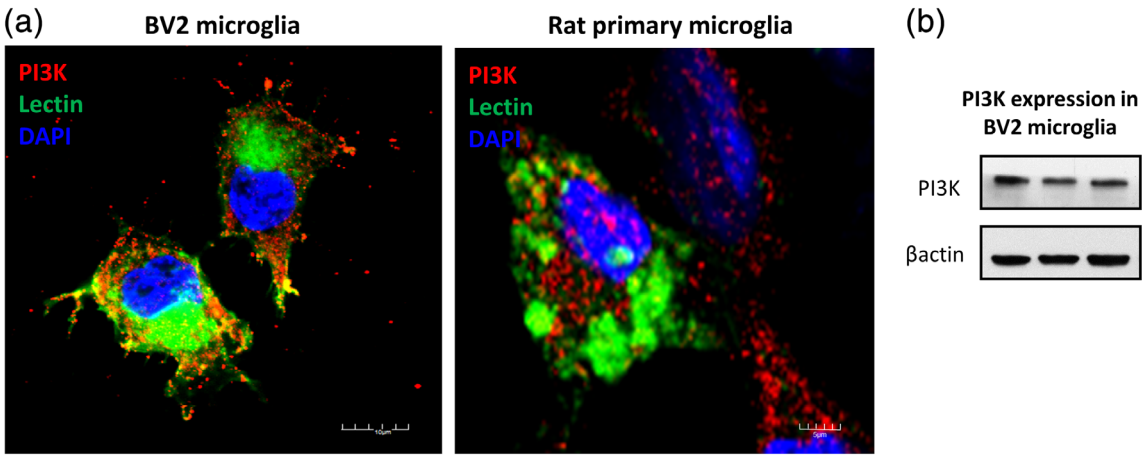

FIGURE 1 PI3K Expression in microglia. (a) Immunocytochemistry images showing the expression of PI3K (red) in both BV2 microglial cell line (left) and rat primary microglia (right). Nuclei are stained blue with DAPI, and microglia are stained green with Lectin. (b) PI3K expression was also confirmed by western blotting. β-Actin was used as an internal control. PI3K, phosphatidylinositol 3-kinase [Color figure can be viewed at wileyonlinelibrary.com]

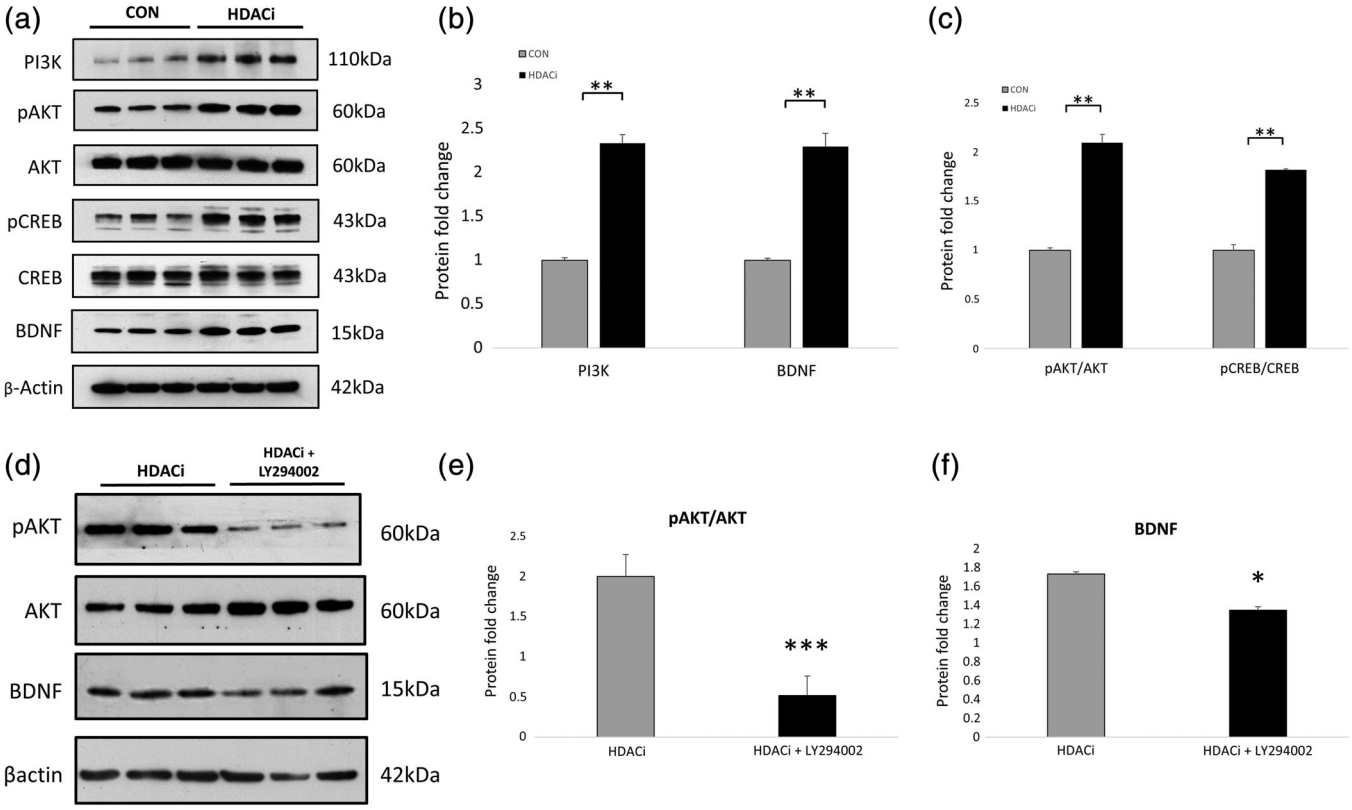

FIGURE 2 HDAC inhibition upregulates PI3K/AKT pathway. (a) Western blot showing the upregulation of PI3K expression (p = .0050), phosphorylation of AKT (p = .0031) and CREB (p = .0011), and also BDNF expression (p = .0154) upon treatment with HDAC inhibitor (NaBu) in BV2 microglial cells, compared to control while the levels of total AKT and CREB remain unchanged. (b) Western blot data were quantified and normalized to β-Actin. (c) Phospho-AKT normalized to total AKT and phospho-CREB normalized to total CREB. (d) Co-treatment of HDAC inhibitor with PI3K inhibitor LY294002, confirmed by significant downregulation of pAKT (p = .0005), resulted in a decrease in BDNF expression (p = .0371). (e, f) Western blot data quantified and normalized to β-Actin, phospho-AKT normalized to total AKT. (n = 3, *p < .05, **p < .01, ***p < .001, compared with control). BDNF, brain-derived neurotrophic factor; CREB, cAMP response element-binding protein; PI3K, phosphatidylinositol 3-kinase

the PI3K inhibitor, LY294002. The results show that when the function of PI3K was blocked (seen by the minimal phosphorylation of AKT, p = .0005), the effects of HDAC inhibition on BDNF expression was also significantly reduced (Figure 2d,f, p = .0372). This confirms that HDAC inhibition affects BDNF expression through PI3K signaling.

Immunofluorescence analysis in rat primary microglia treated with HDACi further confirmed the increase in the expression of PI3K (Figure 3a), pAKT (Figure 3b), pCREB (Figure 3c), and BDNF (Figure 3d) compared to control. These results show that pharmacological inhibition of HDACs by HDAC inhibitor, NaBu, brought about an upregulation of the PI3K/AKT cascade in microglia indicating that microglial PI3K is epigenetically regulated by histone modifications.

We next investigated if the HDACi-induced upregulation of PI3K expression is mediated by a histone acetylation mark. The ChIP assay revealed that HDAC inhibition enhances the enrichment of H3K9ac in the Pik3ca promoter region in microglia treated with HDACi at both 1 hr (p = .0169) and 6 hr (p = .01948) time points (Figure 4). HDAC inhibition increases the overall H3K9ac expression, which promotes the transcription of PI3K. Enhanced expression of PI3K appears to enhance the phosphorylation of AKT, which in turn enhances the phosphorylation of CREB and subsequently the expression of BDNF which has been shown to be involved in synaptic plasticity and transmission.

3.3 | Posttranslational regulation of microglial PI3K by sumoylation

In addition to histone modifications, posttranslational modifications such as sumoylation have also been shown to regulate the expression of PI3K. Sumoylation is a posttranslational modification by small ubiquitin-like modifier (SUMO) proteins involved in processes such as protein stability, nuclear-cytosolic transport, and transcriptional regulation (Han, 2017). It has been shown that SUMO1 binds to PI3K, and sumoylation regulates the PI3K-AKTsignaling pathway (De la Cruz-Herrera et al., 2016). To examine the importance of sumoylation of PI3K by SUMO1, SUMO1 knockdown BV2 microglial stable cell line using shRNA lentiviral vectors was generated. For negative control, cells were transfected with pLKO.1 scrambled shRNA. Immunocytochemistry (Figure 5) and western blot (Figure 6a) analysis confirmed the efficient knockdown of SUMO1 in microglial cells. SUMO 1 expression was evident in control microglial cells transfected with pLKO.1 scrambled shRNA.

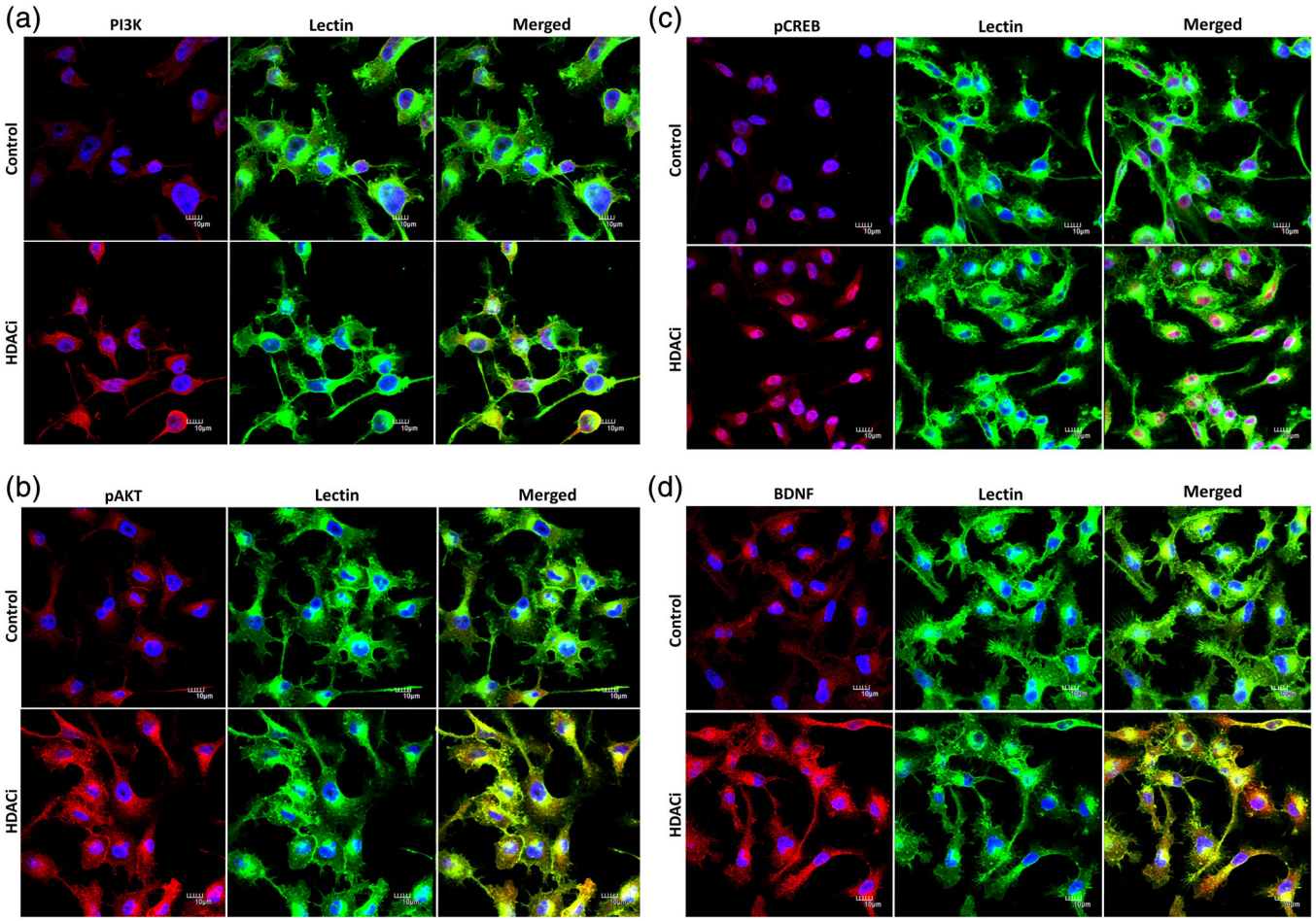

FIGURE 3 HDAC inhibition upregulates PI3K/AKT pathway. Immunocytochemistry images showing an increase in the expression of (a) PI3K (red), (b) phospho-AKT (red), (c) phospho-CREB, and (d) BDNF in rat primary microglia treated with HDAC inhibitor (NaBu) compared to that of control. Nuclei are stained blue with DAPI, and microglia are stained green with Lectin. Scale bar = 10 μm. BDNF, brain-derived neurotrophic factor; CREB, cAMP response element-binding protein; PI3K, phosphatidylinositol 3-kinase [Color figure can be viewed at wileyonlinelibrary.com]

Stable knockdown of SUMO1 in BV2 microglial cells significantly decreased the expression of PI3K (p = .0128), the phosphorylation of AKT (p = .0007) and CREB (p = .0157), and the expression of target protein, BDNF (p = .0209) (Figure 6a,b). We also showed that in addition to the p110α subunit, the p85α subunit of PI3K also shows downregulated expression in SUMO1 knockdown cells (p = .0494) (Supplementary Figure 9). To show that BDNF expression is regulated by PI3K function, we incubated SUMO1 knockdown cells with active PI3K. The rescue in PI3K function was evident as there was a significant increase in the phosphorylation of AKT compared to control (Figure 6d,e, p = .0024) which resulted in a significant upregulation of BDNF expression (Figure 6d,e, p = .0056).

The decrease in expression levels of these proteins was further confirmed at the cellular level by immunocytochemistry (Figure 7a–d). Immunofluorescence analysis revealed that the expression levels of PI3K (Figure 7a), phospho-AKT (Figure 7b), phospho-CREB (Figure 7c), and BDNF (Figure 7d) were lower in SUMO1 knockdown cells compared to that of control cells transfected with pLKO.1 scrambled shRNA. Taken together, these results suggest that microglial PI3K is sumoylated posttranslationally, which in turn regulates its downstream effectors.

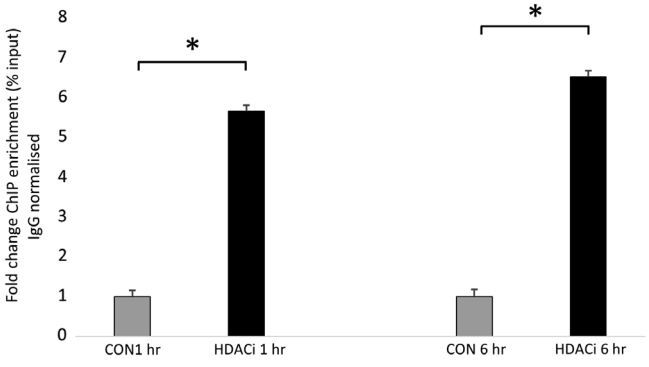

FIGURE 4 Enrichment of acetylation mark in Pik3ca. Chromatin immunoprecipitation (ChIP) assay shows an increase in H3K9ac enrichment in the Pik3ca promoter region upon 1 hr (p = .0169) and 6 hr (p = .01948) treatment with HDACi. Both time points show a significant increase in H3K9ac enrichment in the promoter of PI3K. H3K9ac enrichment was normalized against H3 enrichment to account for nucleosome density at the promoter regions probed. (n = 4, *p < .05, **p < .01, ***p < .001, compared with control). PI3K, phosphatidylinositol 3-kinase

3.4 | PI3K cascade restores plasticity deficit in microglia-ablated CA1 region of hippocampus

As it has been shown in the present study that PI3K-AKT-CREB pathway which regulates BDNF involved in synaptic plasticity is functional in microglial cells, we have investigated the involvement of microglia in LTP. LTP was studied by whole-cell voltage-clamp electrophysiology recordings in the CA1 pyramidal neurons of rat hippocampal slices (Figure 8b) in which microglial cells were selectively ablated or disrupted (Figure 8a) by applying the drug, clodronate (100 μg/mL), while other cell types were unaffected (Supplementary Figure 7).

LTP induction paradigm evoked a robust EPSC potentiation (Figure 8c) in the control slices at the singleneuron level. Statistically significant EPSC potentiation was observed (p = .0156 at 15, 30, and 45 min) for the entire recording period (50 min) after LTP induction. However, there was a lack of LTP, and the EPSC potentiation was attenuated after 19 min, when the LTP was induced in the microglia-ablated hippocampal slices (Figure 8d, p = .0313). The results showed that upon clodronate treatment, there was a significant decline in LTP

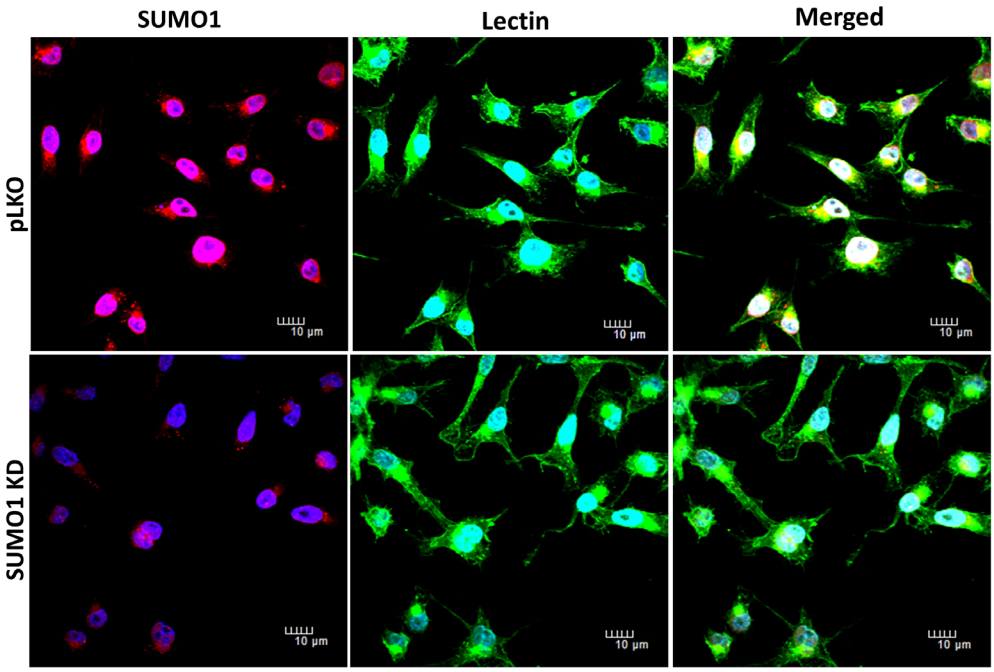

FIGURE 5 SUMO1 knockdown. SUMO1 knockdown BV2 microglial cells generated using SUMO1 shRNA lentiviral vectors were confirmed by immunocytochemistry where SUMO1 is stained in red, microglia are stained green, and DAPI is used to stain the nucleus. Note the decreased expression of SUMO1 in SUMO1 knockdown cells. Scale bar = 10 μm [Color figure can be viewed at wileyonlinelibrary.com]

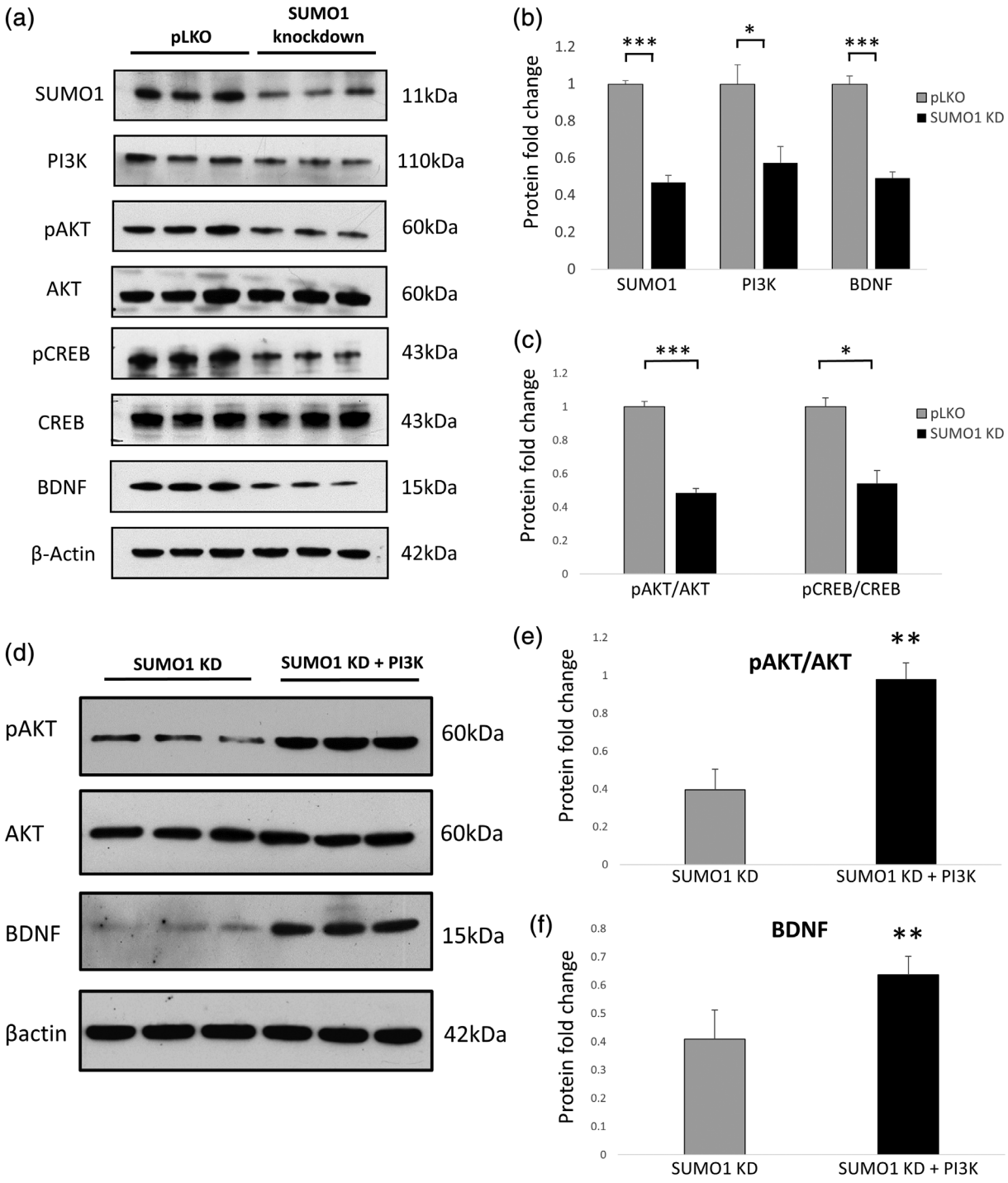

FIGURE 6 SUMO1 Knockdown downregulates PI3K/AKT pathway. (a) Western blot showing the downregulation of PI3K expression ($p = .0128$) and phosphorylation of AKT ($p = .0007$) in SUMO1 knockdown cells while the levels of total AKT remain unchanged. There was also decrease in the phosphorylation of CREB ($p = .0157$) in SUMO1 knockdown cells while the levels of total CREB remain unchanged. The expression of BDNF ($p = .0209$) was also downregulated in SUMO1 knockdown cells. SUMO1 knockdown also confirmed here by western blot ($p = .0005$). (b) Western blot data were quantified and normalized to β-Actin. (c) Phospho-AKT normalized to total AKT and phospho-CREB normalized to total CREB. (d) To restore PI3K function, active PI3K was added to the media leading to a significant increase in AKT phosphorylation ($p = .0024$) followed by a rescue of BDNF induction ($p = .0056$). (e, f) Western blot data quantified and normalized to β-Actin, phospho-AKT normalized to total AKT. ($n = 3$, $^*p < .05$, $^{**}p < .01$, $^{***}p < .001$, compared with control). BDNF, brain-derived neurotrophic factor; CREB, cAMP response element-binding protein; PI3K, phosphatidylinositol 3-kinase

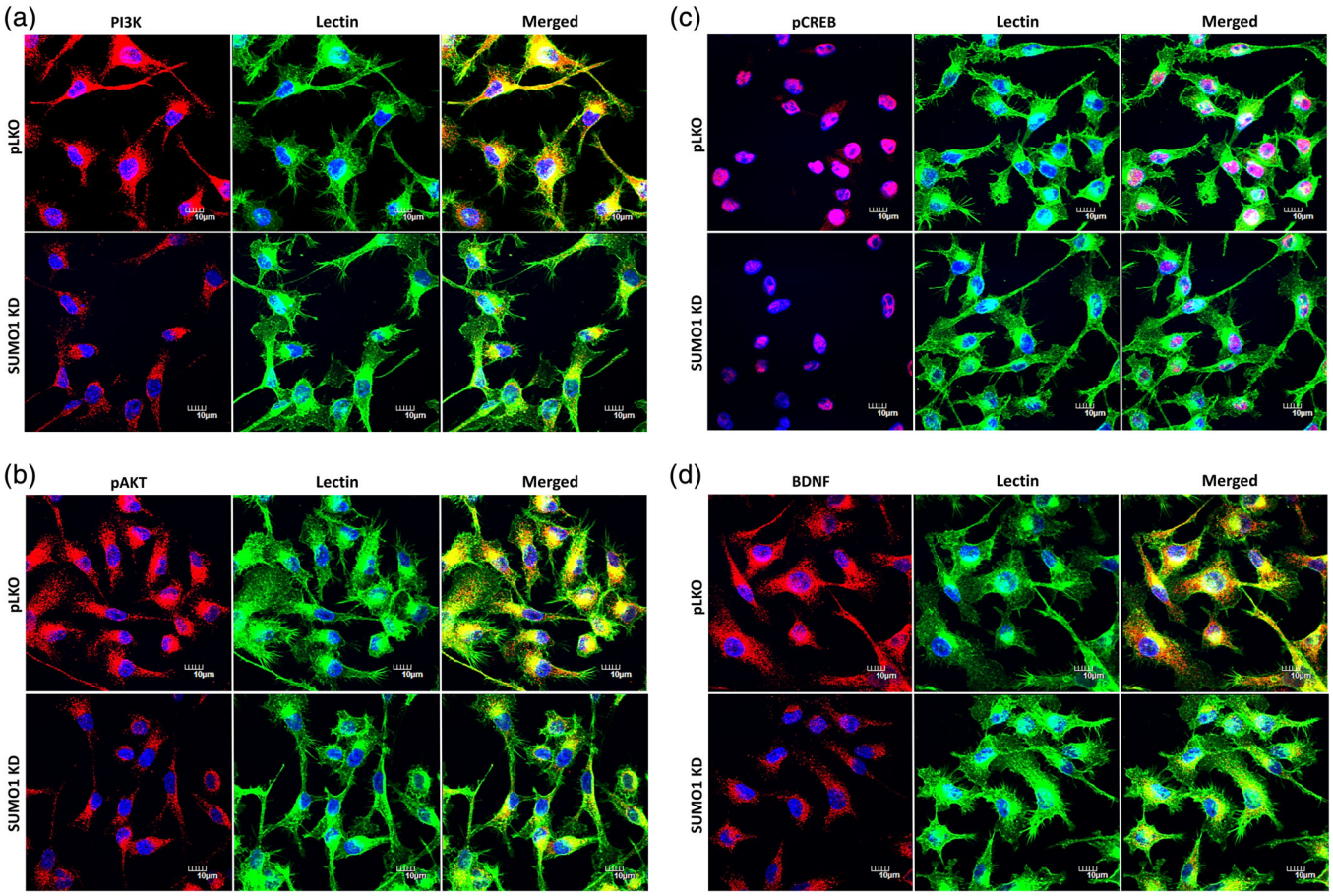

FIGURE 7 SUMO1 knockdown downregulates PI3K/AKT pathway. Immunocytochemistry images showing a decrease in the expression of (a) PI3K (red), (b) pAKT (red), (c) pCREB (red), and (d) BDNF (red) in SUMO1 knockdown cells compared to control. Nuclei are stained blue with DAPI, and microglia are stained green with Lectin. Scale bar = 10 μm. BDNF, brain-derived neurotrophic factor; CREB, cAMP response element-binding protein; PI3K, phosphatidylinositol 3-kinase [Color figure can be viewed at wileyonlinelibrary.com]

(Figure 8d) compared to its own baseline EPSC (p = .0313 at 15 min, p = .4375 at 30 min, p = .6875 at 45 min). This implies that microglia play key roles in neuronal LTP.

To show the involvement of the microglial PI3K/AKT pathway and BDNF on LTP and synaptic plasticity, active PI3K was added to the hippocampal slices after clodronate treatment. Interestingly, the treatment of active PI3K was able to restore the LTP attenuation caused by clodronate (Figure 8e). The EPSC potentiation was significant after the induction of LTP, and the potentiation was maintained for the entire recording period (p = .0078 at 15, 30, and 45 min). Similarly, when BDNF was bath applied to the hippocampal slices after clodronate treatment (Figure 8f), statistically significant LTP was observed after high-frequency stimulation (p = .0078 at 15, 30, and 45 min) for the entire recording period (50 min). This suggests the involvement of microglia, specifically the PI3K/AKT-BDNF cascade in neuronal LTP and synaptic plasticity and that exogenous PI3K and BDNF are able to rescue LTP possibly through both remaining microglia and neurons. The average values of the EPSC slopes (pA/ms) per time point were analyzed using the Wilcoxon signed rank test when compared within the group or the Mann–Whitney U test when data were compared between groups; $p < .05$ was considered statistically significant.

In order to study the involvement of microglia-released factors such as BDNF on LTP, we investigated the effects of conditioned media obtained from control, HDACi-treated, and SUMO1 knockdown BV2 cells (5% vol/vol) on long-term synaptic plasticity in clodronate-treated acute hippocampal slices by field EPSP recording. A two-pathway experimental design in which long-term plasticity was induced in an independent synaptic input (S1) to the hippocampal pyramidal neurons while another independent synaptic input (S2) to the same neuronal population was recorded as control baseline was used. When conditioned media from control BV2 cells was perfused for 120 min before baseline and throughout the recording period in microglia-ablated acute slices, LTP was restored after STET (p = .0022 at 30 min, p = .0022 at 100 min, p = .0368 at 180 min) and the potentiation persisted for the entire recording time point (3 hr) (Supplementary Figure 8c) comparable to control untreated slices in which microglia were still intact (Supplementary Figure 8b). When HDACi-treated BV2 conditioned media was perfused similarly, we observed a significant potentiation (p = .0079 at 30 min, p = .0079 at 100 min, p = .0079 at 180 min) for the entire recording period after strong tetanization (STET; 3 hr; Supplementary Figure 8d). Interestingly, when conditioned media from SUMO1 knockdown BV2 cells was perfused similar to the previous

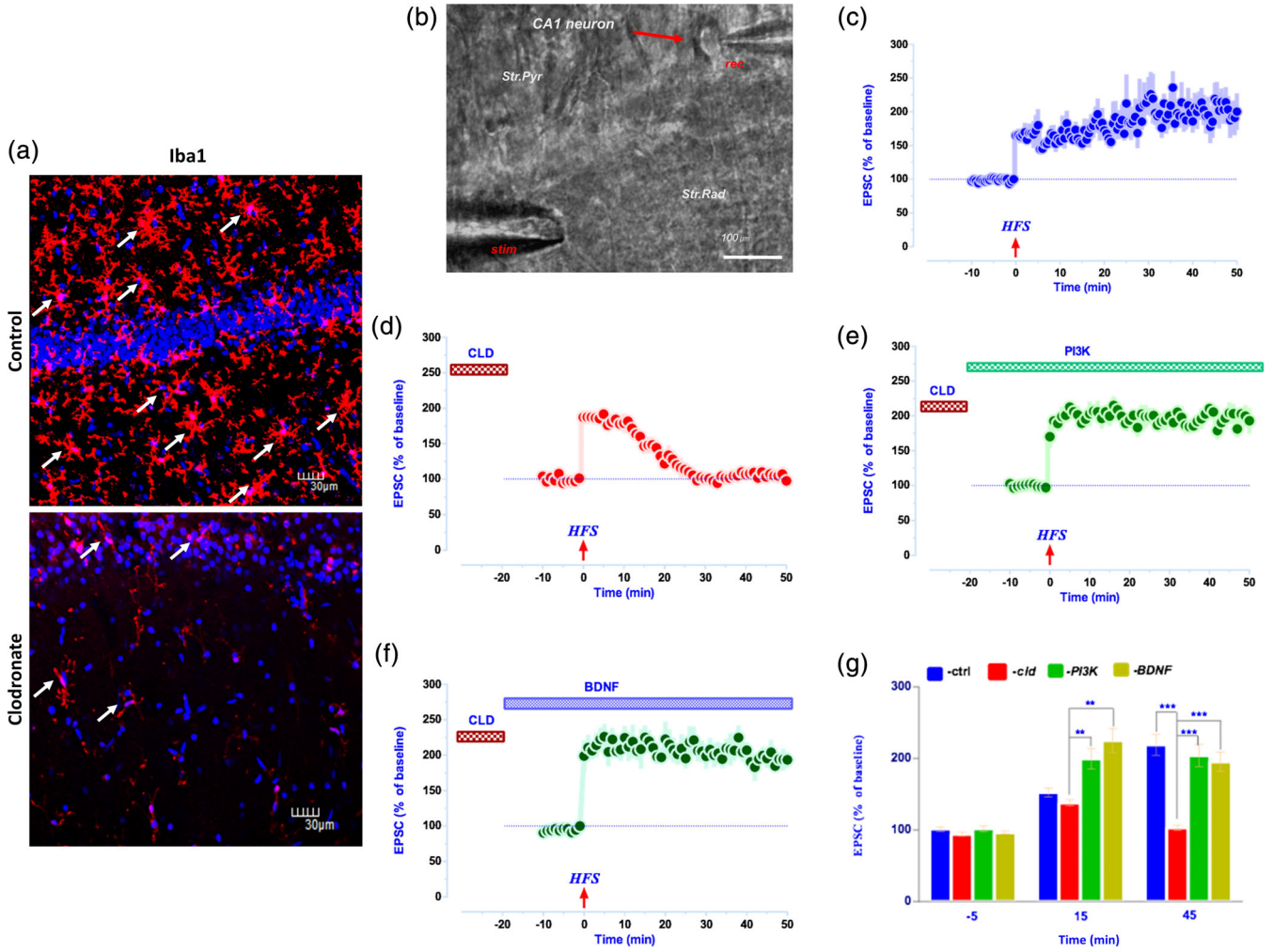

FIGURE 8 Whole-cell patch-clamp electrophysiological recordings showing the effect of microglial ablation on LTP. (a) Immunohistochemistry of hippocampal slices treated with clodronate shows a depletion of microglia in the hippocampal CA1 region. (b) Panel B depicts a hippocampal slice and the relative position of the recording (rec) and stimulating electrode (stim) in the stratum pyramidal (str. Pyr.) and stratum radiatum (str. Rad.), respectively. (c) LTP was induced in a hippocampal slice from a wil-type rat by high-frequency stimulation (HFS) combined with a depolarization to 0 mV 8 min after initial EPSC recording (n = 5). The potentiation of the EPSC slope remained stable the whole period of the recording (50 min). (d) LTP was attenuated when the hippocampal slices were treated with clodronate (100 μg/mL) (n = 6). (e) But when the slices were co-treated with PI3K (1 μg/mL), LTP was restored in the ablated hippocampal slices (n = 8). (f) Similarly, treatment with BDNF (200 ng/mL) could also ameliorate LTP in the clodronate-treated slices. (g) The bar graph summarizes the average values of EPSC slope values during basal activity (−5 min) and 15 and 45 min post-HFS, respectively. Asterisks represent significant difference in the EPSC potentiation between groups (U test). Scale bars for EPSC traces are 50 pA and 40 ms. BDNF, brain-derived neurotrophic factor; LTP, long-term potentiation; PI3K, phosphatidylinositol 3-kinase [Color figure can be viewed at wileyonlinelibrary.com]

experimental conditions, synaptic potentiation was attenuated after 110 min (p = .0087; Supplementary Figure 8e). The percentage of EPSCs at each time point was calculated and analyzed (Supplementary Figure 8f).

4 | DISCUSSION

PI3K has been implicated in synaptic plasticity in neurons (Horwood et al., 2006) by mediating the selective insertion of AMPA receptors at activated synapses during the expression of LTP (Man et al., 2003). The PI3K/AKT pathway has also been implicated in the induction and maintenance of LTP in the hippocampal CA1 region by regulating BDNF, which contributes to synaptic plasticity (Sui et al., 2008). However, PI3K expression in microglia has mainly been shown to be attributed to its role in microglia-mediated inflammation (Sui et al., 2008). The current study demonstrates that PI3K in microglia is regulated by epigenetic factors, undergoes posttranslational modifications, and plays an important role in the maintenance of LTP.

Studies have associated PI3K with HDACs (Ellis et al., 2013; Iaconelli et al., 2017), suggesting that PI3K may be epigenetically regulated by histone modifications. The present study revealed that HDAC inhibition by NaBu upregulated the expression of PI3K in microglia, which is mediated by enhanced enrichment of H3K9ac in

the promoter of PI3K. As the epigenetic regulation by HDACi resulted in upregulation of PI3K expression, the downstream targets of PI3K including AKT, CREB, and BDNF have also been found to be upregulated in microglia. Upon phosphorylation, AKT stimulates the phosphorylation of the nuclear factor, CREB (Du & Montminy, 1998), which in turn regulates the expression of many genes including BDNF in microglia. It has been shown that an increase in the phosphorylation of CREB leads to an increase in the expression of BDNF (Tao, Finkbeiner, Arnold, Shaywitz, & Greenberg, 1998), which has been shown to play a role in synaptic plasticity. In the present study, there was an increase in the expression of phospho-CREB and also an increase in the expression of BDNF in primary microglia exposed to HDACi. Further, we have also confirmed that the effect of HDAC inhibition on BDNF is via PI3K signaling since PI3K inhibition by LY294002, a PI3K inhibitor, significantly diminished BDNF expression in microglia. However, there was no complete blockage of BDNF induction as BDNF expression is known to be regulated by other pathways. This study clearly shows that microglial PI3K affects BDNF expression and inhibition of PI3K function has a significant effect on BDNF expression.

The increase in the expression of PI3K and its downstream targets in microglia upon HDACi treatment was found to be mediated by the enrichment of the histone acetylation mark, H3K9ac in the promoter of PI3K as revealed by ChIP analysis showing significant H3K9ac enrichment in the PI3K promoter after HDACi treatment (Figure 4). Overall, these results suggest that PI3K is epigenetically regulated and that the regulation of PI3K by HDACi is able to alter the expression of its downstream targets, namely, pAKT, pCREB, and ultimately BDNF, which has been shown to play a role in synaptic transmission and plasticity.

Microglial PI3K has also been found to be regulated by sumoylation, which is the posttranslational addition of small ubiquitin-like modifier (SUMO) proteins that regulate cellular processes. PI3K has been shown to be sumoylated in other cell types (De la Cruz-Herrera et al., 2016); however, similar studies have not yet been carried out in microglia. The present study demonstrates that SUMO1 is expressed in microglia and the specific knockdown of SUMO1 brings about changes in the protein expressions of microglial PI3K and its downstream effectors. Stable knockdown of SUMO1 in microglia cells decreased the expression level of PI3K, the phosphorylation of its target proteins, AKT and CREB, and the expression of BDNF, possibly contributing to synaptic plasticity. It has been shown that microglia play an important role in learning and memory by promoting learning-dependent synapse formation through BDNF signaling (Parkhurst et al., 2013). To corroborate our findings that suggest BDNF expression is regulated by PI3K function via the PI3K/AKT pathway, we show that the rescue of PI3K function by the addition of active PI3K (shown as the phosphorylation of AKT) in SUMO1 knockdown cells significantly upregulates BDNF expression. The present study reveals that BDNF signaling in microglia is regulated by PI3K/AKT pathway via histone modifications and sumoylation in PI3K. This indicates that sumoylation and epigenetic mechanisms are the important regulators of microglial PI3K and subsequently synaptic plasticity.

In order to further address if microglial PI3K is directly involved in modulating neuronal LTP, whole-cell voltage-clamp recordings were performed on hippocampal brain slices treated with clodronate, which has been shown to selectively ablate microglia (Figure 8a). The results revealed that the decline in LTP on hippocampal slices treated with clodronate was rescued by the addition of PI3K or BDNF, indicating that microglial BDNF via the PI3K/AKT pathway contributes to neuronal LTP and synaptic plasticity. The decline in LTP on hippocampal slices after clodronate treatment could be due to impaired microglia since only microglial cells showed dystrophic phenotype while other cell types in the hippocampal slice remain unaffected upon treatment of clodronate (Supplementary Figure 7). It is clear that microglial ablation perturbs LTP, which was rescued by the addition of PI3K and BDNF. However, it cannot be ruled out that the rescue of LTP on hippocampal slices after clodronate treatment by addition of exogenous PI3K/BDNF may be mediated via both neuronal and (remaining) microglial pathways to make up for this loss in slices where there is a depletion of microglia.

We have also confirmed that microglia-released factors contribute to neuronal LTP as our field potential electrophysiological recordings show that conditioned media from BV2 microglial cells, which contain microglia-derived soluble factors such as cytokines, chemokines, and growth factors including BDNF, was able to rescue LTP following microglia ablation by clodronate in acute rat hippocampal slices (Supplementary Figure 8). Although the major contribution of neuronal BDNF to LTP is well established, this study confirms that microglial PI3K-AKT-BDNF signaling also contributes to neuronal LTP, emphasizing the importance of microglia–neuron interactions in learning and memory.

A critical component in the formation of plasticity and memory is the synapse specificity, which is achieved through synaptic tagging and capture (STC) (Frey & Morris, 1997). STC is the cellular model of associative memory and is achieved by capturing plasticity-related products (PRPs) from a strongly activated synaptic input to a weakly activated or tagged synaptic input (Frey & Morris, 1997). Stabilization of STC is enabled by tagging and capturing of PRPs within a specific time window. We have reported earlier that BDNF is an important bidirectional PRP, enabling synaptic plasticity persistence in both potentiated and depressed synapses (Sajikumar & Korte, 2011). Thus, our present study provides the first evidence that non-neuronal components such as microglia can also play an important role in the production of PRPs that stabilize synapses for long-term plasticity and cellular memory.

Understanding the mechanisms of microglial PI3K-AKT-BDNF signaling pathway that contributes to neuronal LTP is clinically relevant, since microglia in the aging brain undergo cellular senescence and dystrophic changes (Spittau, 2017; Streit et al., 2009; Von Bernhardi, Eugenín-von Bernhardi, & Eugenín, 2015), which may be associated with age-related cognitive impairment and neurodegeneration. Overall, this study demonstrates that microglial PI3K is epigenetically regulated by histone modifications and post-translationally by sumoylation and that the microglial PI3K pathway is involved in synaptic plasticity via BDNF, a critical PRP for long-term plasticity. Our future study will provide insight into the

mechanisms of synaptic tag-PRP interaction that stabilizes cellular associative plasticity.

DATA AVAILABILITY STATEMENT

The data that support the findings of this study are available from the corresponding author upon reasonable request.

ACKNOWLEDGEMENTS

This work was funded by the NUS Strategic Research Grant (Memory Networks in Rodent and Primate) DPRT/944/09/14 (R185-000-271-646).

ORCID

Tuck Wah Soong https://orcid.org/0000-0002-0876-0325
Sreedharan Sajikumar https://orcid.org/0000-0002-5761-8982
S. Thameem Dheen https://orcid.org/0000-0001-9600-6789

REFERENCES

Beppu, K., Kosai, Y., Kido, M. A., Akimoto, N., Mori, Y., Kojima, Y., … Ifuku, M. (2013). Expression, subunit composition, and function of AMPA-type glutamate receptors are changed in activated microglia; possible contribution of GluA2 (GluR-B)-deficiency under pathological conditions. *Glia*, *61*(6), 881–891.

Bialik, P., & Woźniak, K. (2017). SUMO proteases as potential targets for cancer therapy. *Postepy Higieny i Medycyny Doswiadczalnej (Online)*, *71*, 997–1004.

Datta, M., Staszewski, O., Raschi, E., Frosch, M., Hagemeyer, N., Tay, T. L., … Ziegler-Waldkirch, S. (2018). Histone deacetylases 1 and 2 regulate microglia function during development, homeostasis, and neurodegeneration in a context-dependent manner. *Immunity*, *48*(3), 514–529. e516.

De la Cruz-Herrera, C., Baz-Martínez, M., Lang, V., El Motiam, A., Barbazán, J., Couceiro, R., … Muñoz-Fontela, C. (2016). Conjugation of SUMO to p85 leads to a novel mechanism of PI3K regulation. *Oncogene*, *35*(22), 2873–2880.

Du, K., & Montminy, M. (1998). CREB is a regulatory target for the protein kinase Akt/PKB. *Journal of Biological Chemistry*, *273*(49), 32377–32379.

Du, Y., Liu, P., Xu, T., Pan, D., Zhu, H., Zhai, N., … Li, D. (2018). Luteolin modulates SERCA2a leading to attenuation of myocardial ischemia/reperfusion injury via sumoylation at lysine 585 in mice. *Cellular Physiology and Biochemistry*, *45*(3), 883–898.

Egger, G., Liang, G., Aparicio, A., & Jones, P. A. (2004). Epigenetics in human disease and prospects for epigenetic therapy. *Nature*, *429* (6990), 457–463.

Ellis, L., Ku, S., Ramakrishnan, S., Lasorsa, E., Azabdaftari, G., Godoy, A., & Pili, R. (2013). Combinatorial antitumor effect of HDACs and the PI3K-Akt-mTOR pathway inhibition in a Pten deficient model of prostate cancer. *Oncotarget*, *4*(12), 2225–2236.

Finkbeiner, S., Tavazoie, S. F., Maloratsky, A., Jacobs, K. M., Harris, K. M., & Greenberg, M. E. (1997). CREB: a major mediator of neuronal neurotrophin responses. *Neuron*, *19*(5), 1031–1047.

Frey, U., & Morris, R. G. (1997). Synaptic tagging and long-term potentiation. *Nature*, *385*(6616), 533–536.

Gomes, C., Ferreira, R., George, J., Sanches, R., Rodrigues, D. I., Gonçalves, N., & Cunha, R. A. (2013). Activation of microglial cells triggers a release of brain-derived neurotrophic factor (BDNF) inducing their proliferation in an adenosine a 2A receptor-dependent manner: A 2A receptor blockade prevents BDNF release and proliferation of microglia. *Journal of Neuroinflammation*, *10*(1), 780.

Han, Y. (2017). The localization to PML nuclear bodies and stability of TRAIP/RNF206 are controlled by SUMOylation. *The FASEB Journal*, *31*(1 Suppl), 602.601–602.601.

Hertz, L., & Chen, Y. (2016). All 3 types of glial cells are important for memory formation. *Frontiers in Integrative Neuroscience*, *10*(31), 1–4.

Hong, S., Dissing-Olesen, L., & Stevens, B. (2016). New insights on the role of microglia in synaptic pruning in health and disease. *Current Opinion in Neurobiology*, *36*, 128–134.

Horwood, J. M., Dufour, F., Laroche, S., & Davis, S. (2006). Signalling mechanisms mediated by the phosphoinositide 3-kinase/Akt cascade in synaptic plasticity and memory in the rat. *European Journal of Neuroscience*, *23*(12), 3375–3384.

Iaconelli, J., Lalonde, J., Watmuff, B., Liu, B., Mazitschek, R., Haggarty, S. J., & Karmacharya, R. (2017). Lysine Deacetylation by HDAC6 regulates the kinase activity of AKT in human neural progenitor cells. *ACS Chemical Biology*, *12*(8), 2139–2148.

Jäkel, S., & Dimou, L. (2017). Glial cells and their function in the adult brain: A journey through the history of their ablation. *Frontiers in Cellular Neuroscience*, *11*, 24.

Ji, K., Akgul, G., Wollmuth, L. P., & Tsirka, S. E. (2013). Microglia actively regulate the number of functional synapses. *PLoS One*, *8*(2), e56293.

Jones, P. A., & Baylin, S. B. (2002). The fundamental role of epigenetic events in cancer. *Nature Reviews Genetics*, *3*(6), 415–428.

Kettenmann, H., Kirchhoff, F., & Verkhratsky, A. (2013). Microglia: New roles for the synaptic stripper. *Neuron*, *77*(1), 10–18.

Kim, Y.-I. (2005). Nutritional epigenetics: Impact of folate deficiency on DNA methylation and colon cancer susceptibility. *The Journal of Nutrition*, *135*(11), 2703–2709.

Koellhoffer, E., Grenier, J., Ritzel, R., & McCullough, L. (2015). Abstract T P80: Inhibition of Ezh2 leads to decreased M1 and enhanced M2 microglia phenotypes. *Stroke*, **46**, Suppl 1.

Krishna, K., Behnisch, T., & Sajikumar, S. (2016). Inhibition of histone deacetylase 3 restores amyloid-β oligomer-induced plasticity deficit in hippocampal CA1 pyramidal neurons. *Journal of Alzheimer's Disease*, *51*(3), 783–791.

Mallilankaraman, K., Cárdenas, C., Doonan, P. J., Chandramoorthy, H. C., Irrinki, K. M., Golenár, T., … Müller, M. (2012). MCUR1 is an essential component of mitochondrial Ca2+ uptake that regulates cellular metabolism. *Nature Cell Biology*, *14*(12), 1336–1343.

Mallilankaraman, K., Doonan, P., Cárdenas, C., Chandramoorthy, H. C., Müller, M., Miller, R., … Birnbaum, M. J. (2012). MICU1 is an essential gatekeeper for MCU-mediated mitochondrial Ca 2+ uptake that regulates cell survival. *Cell*, *151*(3), 630–644.

Man, H.-Y., Wang, Q., Lu, W.-Y., Ju, W., Ahmadian, G., Liu, L., … Lu, J. (2003). Activation of PI3-kinase is required for AMPA receptor insertion during LTP of mEPSCs in cultured hippocampal neurons. *Neuron*, *38*(4), 611–624.

Mayford, M., Siegelbaum, S. A., & Kandel, E. R. (2012). Synapses and memory storage. *Cold Spring Harbor Perspectives in Biology*, *4*(6), a005751.

Moosavi, A., & Ardekani, A. M. (2016). Role of epigenetics in biology and human diseases. *Iranian Biomedical Journal*, *20*(5), 246–258.

Neves, G., Cooke, S. F., & Bliss, T. V. (2008). Synaptic plasticity, memory and the hippocampus: A neural network approach to causality. *Nature Reviews Neuroscience*, *9*(1), 65–75.

Norden, D. M., & Godbout, J. P. (2013). Microglia of the aged brain: Primed to be activated and resistant to regulation. *Neuropathology and Applied Neurobiology*, *39*(1), 19–34.

Parkhurst, C. N., Yang, G., Ninan, I., Savas, J. N., Yates, J. R., Lafaille, J. J., … Gan, W.-B. (2013). Microglia promote learning-dependent synapse formation through brain-derived neurotrophic factor. *Cell*, *155*(7), 1596–1609.

Park-Sarge, O.-K., & Sarge, K. D. (2008). Detection of sumoylated proteins. In *The Nucleus*: Hancock, Ronald (Ed.) *Volume 2: Chromatin, Transcription, Envelope, Proteins, Dynamics, and Imaging*. New Jersey, USA: Humana Press (pp. 255–265).

Pfeiffer, T., Avignone, E., & Nägerl, U. V. (2016). Induction of hippocampal long-term potentiation increases the morphological dynamics of microglial processes and prolongs their contacts with dendritic spines. *Scientific Reports*, *6*, 32422.

Sajikumar, S., & Korte, M. (2011). Metaplasticity governs compartmentalization of synaptic tagging and capture through brain-derived neurotrophic factor (BDNF) and protein kinase Mζ (PKMζ). *Proceedings of the National Academy of Sciences*, *108*(6), 2551–2556.

Saura, J., Tusell, J. M., & Serratosa, J. (2003). High-yield isolation of murine microglia by mild trypsinization. *Glia*, *44*(3), 183–189.

Schafer, D. P., Lehrman, E. K., & Stevens, B. (2013). The "quad-partite" synapse: Microglia-synapse interactions in the developing and mature CNS. *Glia*, *61*(1), 24–36.

Slepko, N., Patrizio, M., & Levi, G. (1999). Expression and translocation of protein kinase C isoforms in rat microglial and astroglial cultures. *Journal of Neuroscience Research*, *57*(1), 33–38.

Spittau, B. (2017). Aging microglia—Phenotypes, functions and implications for age-related neurodegenerative diseases. *Frontiers in Aging Neuroscience*, *9*, 194.

Stebbing, M. J., Cottee, J. M., & Rana, I. (2015). The role of ion channels in microglial activation and proliferation—A complex interplay between ligand-gated ion channels, K+ channels, and intracellular Ca2+. *Frontiers in Immunology*, *6*, 497.

Streit, W. J., Braak, H., Xue, Q.-S., & Bechmann, I. (2009). Dystrophic (senescent) rather than activated microglial cells are associated with tau pathology and likely precede neurodegeneration in Alzheimer's disease. *Acta Neuropathologica*, *118*(4), 475–485.

Sui, L., Wang, J., & Li, B.-M. (2008). Role of the phosphoinositide 3-kinase-Akt-mammalian target of the rapamycin signaling pathway in long-term potentiation and trace fear conditioning memory in rat medial prefrontal cortex. *Learning & Memory*, *15*(10), 762–776.

Takeuchi, T., Duszkiewicz, A. J., & Morris, R. G. (2014). The synaptic plasticity and memory hypothesis: Encoding, storage and persistence. *Philosophical Transactions of the Royal Society B*, *369*(1633), 20130288.

Tao, X., Finkbeiner, S., Arnold, D. B., Shaywitz, A. J., & Greenberg, M. E. (1998). Ca 2+ influx regulates BDNF transcription by a CREB family transcription factor-dependent mechanism. *Neuron*, *20*(4), 709–726.

Tremblay, M.-È., & Majewska, A. K. (2011). A role for microglia in synaptic plasticity? *Communicative & Integrative Biology*, *4*(2), 220–222.

Von Bernhardi, R., Eugenín-von Bernhardi, L., & Eugenín, J. (2015). Microglial cell dysregulation in brain aging and neurodegeneration. *Frontiers in Aging Neuroscience*, *7*, 124.

Welberg, L. (2014). Synaptic plasticity: A synaptic role for microglia. *Nature Reviews Neuroscience*, *15*(2), 68.

Wu, Y., Dissing-Olesen, L., MacVicar, B. A., & Stevens, B. (2015). Microglia: Dynamic mediators of synapse development and plasticity. *Trends in Immunology*, *36*(10), 605–613.

Yang, W., Sheng, H., & Wang, H. (2016). Targeting the SUMO pathway for neuroprotection in brain ischaemia. *Stroke and Vascular Neurology*, *1*(3), 101–107.

Zhao, R., Hu, W., Tsai, J., Li, W. & Gan, W. B. (2017). Microglia limit the expansion of β-amyloid plaques in a mouse model of Alzheimer's disease. *Molecular neurodegeneration*, *12*(1), 47.

SUPPORTING INFORMATION

Additional supporting information may be found online in the Supporting Information section at the end of this article.

How to cite this article: Saw G, Krishna K, Gupta N, et al. Epigenetic regulation of microglial phosphatidylinositol 3-kinase pathway involved in long-term potentiation and synaptic plasticity in rats. *Glia*. 2020;68:656–669. https://doi.org/10.1002/glia.23748